Inorg. Chem. **2007**, *46*, 10501–10509

Structural and Thermodiffractometric Analysis of Coordination Polymers. Part II:[1] Zinc and Cadmium Derivatives of the Bim ligand [Bim = Bis(1-imidazolyl)methane]

Norberto Masciocchi,*,† Claudio Pettinari,*,‡ Enrica Alberti,† Riccardo Pettinari,‡ Corrado Di Nicola,‡ Alessandro Figini Albisetti,§ and Angelo Sironi§

Dipartimento di Scienze Chimiche e Ambientali, Università dell'Insubria, via Valleggio 11, 22100 Como, Italy, Dipartimento Scienze Chimiche, Università di Camerino, via S. Agostino 1, 62032 Camerino, Italy, and Dipartimento di Chimica Strutturale e Stereochimica Inorganica, Università di Milano, via Venezian 21, 20133 Milano, Italy

Received August 1, 2007

New polynuclear coordination species containing the ditopic bis(1-imidazolyl)methane (Bim) ligand have been prepared as microcrystalline powders and structurally characterized by ab initio X-ray powder diffraction methods. $[Zn(CH_3COO)_2(Bim)]_n$ contains 1D chains with tetrahedral metal atoms bridged by Bim ligands; $[CdBr_2(Bim)]_n$ shows a dense packing with hexacoordinated Cd(II) ions and μ-Br and μ-Bim bridges; at variance, the isomorphous $[ZnCl_2(Bim)]_n$ and $[ZnBr_2(Bim)]_n$ species contain cyclic dimers based on tetrahedral Zn(II) ions. Thermodiffractometric analysis allowed estimation of the linear thermal expansion coefficients and strain tensors derived there from. Bim-rich phases, with 2:1 ligand-to-metal ratio, were also isolated: $ZnBr_2(Bim)_2(H_2O)_3$ and $[Cd(CH_3COO)_2(Bim)_2]_n$ containing cis and trans MN_4O_2 chromophores, respectively, show 1D polymers built upon M_2Bim_2 cycles, hinged on the metal ions. In all species the conformation of the Bim ligands is C_s (or nearly so), while in the few sparse reports of similar coordination polymers the alternative C_2 one was preferentially observed.

Introduction

Group 12 coordination polymers have recently attracted the interest of material scientists in a number of newly emerging fields for their versatile chemistry and, in several cases, appealing functional properties. For example, porous zinc polycarboxylates[2] and even the simple zinc formate[3] have shown interesting gas sorption properties; zinc bisimidazolate[4] has been proposed as a new material with dielectric properties superior to the widely used SiO_2 and PTFE (Teflon); zinc pyrazolate,[5] zinc imidazolate,[6] and zinc pyrimidin-2-olate[7] polymers have shown thermal stability up to 550 °C; finally, polynuclear zinc and cadmium coordination compounds are attractive luminescent materials.[8]

Following our previous studies on zinc and cadmium derivatives with exo-bidentate nitrogen ligands,[9] we have now prepared polynuclear coordination species with the Bim ligand (Bim = bis(1-imidazolyl)methane, see Chart 1), a ditopic ligand rarely[10] employed in the formation of coordination polymers; this ligand,[11] which we consider a larger analogue of widely used N,N′-exobidentate fragments with bent coordination geometry (such as pyrazolates, imidazolates, pyrimidines, and their derivatives), is here coupled with group 12 ions in search for new species,

* To whom correspondence should be addressed. E-mail: angelo.sironi@unimi.it.
† Università dell'Insubria.
‡ Università di Camerino.
§ Università di Milano.

(1) Part I: Masciocchi, N.; Pettinari, C.; Alberti, E.; Pettinari, R.; Di Nicola, C.; Figini Albisetti, A.; Sironi, A. *Inorg. Chem.* **2007**, *46*, 10491−10500.
(2) Li, H.; Eddaoudi, M.; O'Keeffe, M.; Yaghi, O. *Nature* **1999**, *402*, 276−279.
(3) Wang, Z.; Zhang, Y.; Kurmoo, M.; Liu, T.; Vilminot, S.; Zhao, B.; Gao, S. *Aust. J. Chem.* **2006**, *59*, 617−628.
(4) Świątek-Tran, B.; Kołodziej, H. A.; Tran, V. H. J. *Solid State Chem.* **2004**, *177*, 1011−1016.
(5) Sironi, A.; Masciocchi, N.; Ardizzoia, G. A.; Lamonica, G.; Maspero, A. *Inorg. Chem.* **1999**, *38*, 3657−3664.
(6) Park, K. S.; Ni, Z.; Côté, A. P.; Choi, J. Y.; Huang, R.; Uribe-Romo, F. J.; Chae, H. K.; O'Keeffe, M.; Yaghi, O. M. *PNAS* **2006**, *103*, 10186−10191.
(7) Masciocchi, N.; Ardizzoia, G. A.; Lamonica, G.; Maspero, A.; Sironi, A. *Eur. J. Inorg. Chem.* **2000**, 2507−2515.
(8) Zheng, S. L.; Chen, X. M. *Aust. J. Chem.* **2004**, *57*, 703−712.
(9) Masciocchi, N.; Galli, S.; Sironi, A.; Cariati, E.; Galindo, M. A.; Barea, E.; Romero, M. A.; Salas, J. M.; Navarro, J. A. R.; Santoyo-González, F. *Inorg. Chem.* **2006**, *45*, 7612−7620. Masciocchi, N.; Galli, S.; Alberti, E.; Sironi, A.; Di Nicola, C.; Pettinari, C.; Pandolfo, L. *Inorg. Chem.* **2006**, *45*, 9064−9074.

10.1021/ic7015319 CCC: $37.00
Published on Web 11/15/2007

Chart 1

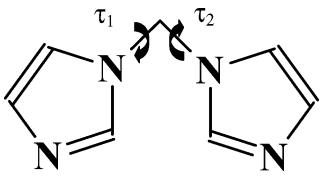

Chart 2

$[ZnCl_2(Bim)]_n$	**1**
$[ZnBr_2(Bim)]_n$	**2**
$ZnBr_2(Bim)\cdot 3H_2O$	**3**
$[Zn(CH_3COO)_2(Bim)]_n$	**4**
$Cd_2Cl_4(Bim)_2(H_2O)(EtOH)$	**5**
$[CdBr_2(Bim)]_n$	**6**
$CdBr_2(Bim)_2(H_2O)(MeOH)$	**7**
$[Cd(CH_3COO)_2(Bim)_2]_n$	**8**

possibly exhibiting one or more of the functional properties described above, with particular emphasis on the possibility of detecting porous species capable of selective gas sorption. To the best of our knowledge, only one report of zinc and cadmium derivatives of Bim has appeared in the literature with perchlorate and azido counterions,[10a] while in the following we report on species prepared by employing metal halides or acetates.

Given that these materials only precipitated as polycrystalline powders, conventional structural analyses were not viable; therefore, we immediately resorted to ab initio powder diffraction methods,[12] which, in the past decade, allowed us[13] (and others[14]) to unravel the structural features of many coordination polymers, and the discovery of new stoichiometries, connectivity, and polymorphic materials.

In addition, using a custom-made sample heater we followed the thermal evolution of the lattice metrics, aiming at obtaining dynamic information through analysis of static measurements done at constant temperatures.

In order to facilitate the comprehension of the following sections, Chart 2 synoptically contains the chemical formulas and numbering scheme used throughout this contribution.

Experimental Section

Materials and Methods. All chemicals and reagents were of reagent-grade quality and used as received without further purification. All solvents were distilled prior to use. THF and light petroleum (310−333 K) were dried by refluxing over freshly cut sodium. Dichloromethane was freshly distilled from CaH_2. Other solvents were dried and purified by standard procedures. Due to the use of hydrated salts and even if anhydrous and distilled solvents have been employed, most reactions were performed in air, thus allowing, occasionally, the recovery of hydrated polymers for rapid moisture absorption. The samples were dried in vacuo to constant weight (293 K, 0.1 Torr). Elemental analyses were carried out in house with a Fisons Instruments 1108 CHNSO-elemental analyzer. IR spectra from 4000 to 150 cm^{-1} were recorded with a Perkin-Elmer System 2000 FT-IR instrument. ^1H and $^{13}C\{^1H\}$ NMR solution spectra were recorded on a Varian Oxford AS400 NMR spectrometer (400 MHz for ^1H and 100 MHz for ^{13}C). Referencing is relative to TMS (^1H and ^{13}C). NMR samples were prepared by dissolving a suitable amount of compound in 0.5 mL of solvent. Solid-state ^{13}C CP-MAS NMR spectra were recorded using a Bruker AVANCE 400 spectrometer equipped with a 4 mm double-bearing MAS probe. ^{13}C cross-polarization magic-angle spinning (CPMAS) spectra were recorded using a recycle time of 10 s, contact times of 1 ms, and a spinning rate of 5 kHz. The spectra were recorded at room temperature and transformed using a line broadening of 20 Hz.

Solution NMR spectra of the original polymeric species demonstrate that breaking of some metal−ligand bonds and consequent dissociation of the polymer occurs. At variance, in the case of dinuclear species, the reported NMR chemical shifts in $CDCl_3$ witness the persistence of these complexes even in solution.

Syntheses. Synthesis of the Bim ligand is reported in the previous paper (Part I[1]).

$[ZnCl_2(Bim)]_2$ (1). An ethanol solution (20 mL) containing $ZnCl_2\cdot 2H_2O$ (0.172 g, 1.0 mmol) and Bim (0.148 g, 1.0 mmol) was stirred for 24 h at room temperature. The resulting colorless precipitate was isolated by filtration and dried in vacuo. The residue obtained was washed with 5 mL of ethanol and shown to be compound **1** (0.200 g, 0.70 mmol, yield 70%). Mp 346−7 °C (dec). Anal. Calcd for $C_7H_8Cl_2N_4Zn$: C, 29.56; H, 2.83; N, 19.70. Found: C, 29.87; H, 3.01; N, 20.01. IR (Nujol, cm^{-1}): 3391br, 3156w, 3126m, 1694br, 1663br, 1530m, 1520m, 384w, 367w, 313s, 290s ν(Zn−Cl), 225m. ^1H NMR (DMSO-d_6, 293 K): δ 6.22, 6.28 (2s, 2H, CH_{2Bim}), 6.90, 6.94 (2s, 2H, CH_{Bim}), 7.42, 7.51 (2pd, 2H, CH_{Bim}), 7.99, 8.14 (2 pd, 2H, CH_{Bim}).

$[ZnBr_2(Bim)]_2$ (2). An ethanol solution (20 mL) containing $ZnBr_2$ (0.225 g, 1.0 mmol) and Bim (0.148 g, 1.0 mmol) was stirred for 24 h at room temperature. The resulting colorless precipitate was isolated by filtration and dried in vacuo. The residue obtained was washed with 5 mL of ethanol and shown to be compound **2** (0.150 g, 0.40 mmol, yield 40%). Mp > 350 °C (dec). Anal. Calcd for $C_7H_8Br_2N_4Zn$: C, 22.52; H, 2.16; N, 15.01. Found: C, 23.00; H, 2.23; N, 14.98. IR (Nujol, cm^{-1}): 3150m, 3122m, 3005w, 1702br, 1683br, 1606br, 1530s, 1520m, 261s, 229m. ^1H NMR (DMSO-d_6, 293 K): δ 6.37 (s, 2H, CH_{2Bim}), 7.07 (s, 2H, CH_{Bim}), 7.66 (pd, 2H, CH_{Bim}), 8.37 (pd, 2H, CH_{Bim}).

$ZnBr_2(Bim)\cdot 3H_2O$ (3). An ethanol solution (20 mL) containing $ZnBr_2$ (0.225 g, 1.0 mmol) and Bim (0.300 g, 2.0 mmol) was stirred for 24 h at room temperature. The resulting colorless precipitate was isolated by filtration and dried in vacuo. The residue obtained was washed with 5 mL of ethanol and shown to be compound **3** (0.450 g, 0.79 mmol, yield 79%). Mp > 300 °C (dec). Anal. Calcd for $C_{14}H_{22}Br_2N_8O_3Zn$: C, 29.37; H, 3.88; N 19.59. Found: C, 29.62; H, 3.97; N, 19.27. IR (Nujol, cm^{-1}): 3150m, 3122m, 3005w, 1702br, 1683br, 1606br, 1530s, 1520m, 382w, 367w, 296w, 242s, 233s, 226s. ^1H NMR (DMSO-d_6, 293 K): δ 6.37 (s, 2H, CH_{2Bim}), 7.07 (s, 2H, CH_{Bim}), 7.66 (pd, 2H, CH_{Bim}), 8.37 (pd, 2H, CH_{Bim}).

(10) (a) Cui, G. H.; Li, J. R.; Tian, J. L.; Bu, X. H.; Batten, S. R. *Cryst. Growth Des.* **2005**, *5*, 1775−1780. (b) Cui, G. H.; Dong, G. Y.; Ribas, J. *Acta Crystallogr., Sect E: Struct. Rep. Online* **2006**, *62*, m523. (c) Dong, G. Y.; Cui, G. H.; Wang, S. C. *Acta Crystallogr., Sect E: Struct. Rep. Online* **2006**, *62*, m606. (d) Jin, C. M.; Lu, H.; Wu, L. Y.; Huang, J. *Chem. Commun.* **2006**, 5039−5041. (e) Hwang, I. C.; Chandran, R. P.; Singh, N. J.; Khandelwal, M.; Thangadurai, T. D.; Lee, J. W.; Chang, J. A.; Kim, K. S. *Inorg. Chem.* **2006**, *45*, 8062−8069.
(11) Li, J. *Acta Crystallogr., Sect E: Struct. Rep. Online* **2006**, *62*, o1798.
(12) Langford, J. I.; Louër, D. *Rep. Prog. Phys.* **1996**, *59*, 131−234. Porob, D. G.; Row, T. N. G. *Proc. Indian Acad. Sci. (Chem. Sci.)* **2001**, *113*, 435−444.
(13) Masciocchi, N.; Galli, S.; Sironi, A. *Comments Inorg. Chem.* **2005**, *26*, 1−37.
(14) IUCr Commission for Powder Diffraction. *Newsletters #31: Powder Diffraction of Functional Materials*; Masciocchi, N., Ed.; International Union of Crystallography: Chester, U.K., 2004.

Table 1. Crystal Data and Structure Refinement Parameters for the Zinc Derivatives **1**−**4**

	1	**2**	**3**	**4**
empirical formula	$C_{14}H_{16}Cl_4N_8Zn_2$	$C_{14}H_{16}Br_4N_8Zn_2$	$C_{14}H_{16}Br_2N_8O_3Zn$	$C_9H_{11}N_4O_2Zn$
fw	568.93	746.74	569.54	272.60
cryst syst	monoclinic	monoclinic	orthorhombic	triclinic
space Group	$P2_1/c$	$P2_1/c$	Pccn	$P\bar{1}$
unit cell dimensions				
a (Å)	8.6691(3)	8.8912(2)	8.7496(1)	8.402(1)
b (Å)	8.7338(3)	8.8716(2)	13.9514(2)	10.679(2)
c (Å)	14.496(1)	14.8592(3)	16.4736(2)	9.356(1)
α, deg	90	90	90	114.378(8)
β, deg	98.906(3)	97.442(2)	90	91.337(6)
γ, deg	90	90	90	64.980(6)
V (Å^3)	1084.3(1)	1162.20(5)	2010.92(5)	681.1(2)
Z	2	2	4	2
D_c (Mg m^{-3})	1.743	2.134	1.881	1.623
abs coeff (mm^{-1})	7.414	10.744	6.655	2.710
F(000)	568.0	712.0	1120.0	340.0
2θ range	9−105	9−105	5−105	8−105
indexing Gof	25.9	43.3	28.4	18.4
R_p, R_{wp}	0.010, 0.069	0.061, 0.079	0.067, 0.049	0.080, 0.103
R_{Bragg}	0.027	0.023	0.037	0.035
goodness-of-fit	7.08	1.25	6.99	2.30

$[Zn(CH_3COO)_2(Bim)]_n$ (4). An ethanol solution (20 mL) containing $Zn(CH_3COO)_2 \cdot 2H_2O$ (0.219 g, 1.0 mmol) and Bim (0.148 g, 1.0 mmol) was stirred for 24 h at room temperature. The resulting colorless precipitate was isolated by filtration and dried in vacuo. The residue obtained was washed with 5 mL of ethanol and shown to be compound **4** (0.300 g, 0.91 mmol, yield 91%), insoluble in DMSO, DMF acetone, MeCN alcohols, $CHCl_3$, CH_2Cl_2. Mp 316 °C (dec). Anal. Calcd for $C_{11}H_{14}N_4O_4Zn$: C, 39.84; H, 4.26; N, 16.89. Found: C, 39.65; H, 4.23; N, 16.65. IR (Nujol, cm^{-1}): 3153m, 3124m, 3010w, 3005w (CH), 1616s (CO), 1538m, 1512m, 1392s, 510w, 491w, 392m, 368w, 311sh, 300br, 243m.

$Cd_2Cl_4(Bim)_2(H_2O)(EtOH)$ (5). An ethanol solution (20 mL) containing $CdCl_2$ (0.183 g, 1.0 mmol) and Bim (0.148 g, 1.0 mmol) was stirred for 24 h at room temperature. The resulting colorless precipitate was isolated by filtration and dried in vacuo. The residue obtained was washed with 5 mL of ethanol and shown to be compound **5** (0.200 g, 0.70 mmol, yield 70%). Mp 290 °C (dec). Anal. Calcd for $C_{23}H_{32}Cd_2Cl_4N_{12}O_2$: C, 31.51; H, 3.68; N, 19.18. Found: C, 31.55; H, 3.72; N, 19.52. IR (Nujol, cm^{-1}): 3418br, 3101m, 1621br, 1523m, 1494m, 389w, 229w, 208m ν(Cd−Cl), 225m.

$[CdBr_2(Bim)]_n$ (6). An ethanol solution (20 mL) containing $CdBr_2$ (0.272 g, 1.0 mmol) and Bim (0.148 g, 1.0 mmol) was stirred for 24 h at room temperature. The resulting colorless precipitate was isolated by filtration and dried in vacuo. The residue obtained was washed with 5 mL of ethanol and shown to be compound **6** (0.300 g, 0.71 mmol, yield 71%). Mp > 350 °C (dec). Anal. Calcd for $C_7H_8Br_2CdN_4$: C, 20.00; H, 1.92; N, 13.33. Found: C, 20.45; H, 2.08; N, 13. IR (Nujol, cm^{-1}): 3125w, 3118m, 3000w, 1680br, 1520s, 1500s, 392w, 300w, 279w, 253v w, 246vw.

$CdBr_2(Bim)_2(H_2O)(MeOH)$ (7). A methanol solution (20 mL) containing $CdBr_2$ (0.272 g, 1.0 mmol) and Bim (0.296 g, 2.0 mmol) was stirred for 24 h at room temperature. The resulting colorless precipitate was isolated by filtration and dried in vacuo. The residue obtained was washed with 5 mL of methanol and shown to be compound **7** (0.300 g, 0.71 mmol, yield 71%). Mp 312−3 °C (dec). Anal. Calcd for $C_{15}H_{22}Br_4Cd_2N_8O_2$: C, 29.12; H, 3.58; N, 18.11. Found: C, 29.30; H, 3.43; N, 18.00. IR (Nujol, cm^{-1}): 3125w, 3118m, 3000w, 1680br, 1520s, 1500s, 392w, 300w, 279w, 253vw, 246vw. The recovered material, although of high chemical purity, gave only broad diffraction peaks, thus hampering the definition of any reliable (crystalline or molecular) structural model.

$[Cd(CH_3COCH_3COOO)_2(Bim)]_n$ (8). An ethanol solution (20 mL) containing $Cd(ac)_2 \cdot 2H_2O$(0.266 g, 1.0 mmol) and Bim (0.296 g, 1.0 mmol) was stirred for 24 h at room temperature. The resulting colorless precipitate was isolated by filtration and dried in vacuo. The residue obtained was washed with 5 mL of ethanol and shown to be compound **8** (0.350 g, 0.66 mmol, yield 66%), insoluble in DMSO, DMF acetone, MeCN alcohols, $CHCl_3$, and CH_2Cl_2 and soluble in D_2O. Mp 252−4 °C (dec). Anal. Calcd for $C_{18}H_{22}N_8O_4Cd$: C, 41.04; H, 4.21; N, 21.27. Found: C, 41.12; H, 4.12; N, 20.98. IR (Nujol, cm^{-1}): 3140w, 3096m (CH), 1664s, 1595sh, 1582s, 1500m, 1380s (CO), 469w, 390w, 303m, 281w. ^{1}H NMR (D_2O, 293 K): δ 1.72 (s, 6H, CH_3) 6.11 (s, 4H, CH_{2Bim}), 6.87 (s, 4H, CH_{Bim}), 7.15 (br, 4H, CH_{Bim}), 7.75 (br, 4H, CH_{Bim}).

X-ray Powder Diffraction Structural Analysis. Diffraction data for compounds **2**, **4**, and **6** were recorded on a Bruker AXS D8 Advance diffractometer operating in the θ:θ mode equipped with a secondary beam graphite monochromator, a Na(Tl)I scintillation counter, and pulse-height amplifier discrimination. Slits used: DS 0.5°, AS 0.5°, RS 0.1 mm. The remaining polycrystalline powders were measured with a PSD Lynxeye detector and DS 0.5°. Cu Kα radiation: $\lambda = 1.5418$ Å; generator setting 40 kV, 40 mA. Gently ground powders were deposited in the hollow of a quartz zero-background plate supplied by The Gem Dugout (Swarthmore, PA). For **2**, **4**, and **6**: step scan mode, with $5 < 2\theta < 105°$, $\Delta 2\theta = 0.02°$, $t = 15$ s step^{-1}. For the others: continuous mode, with $5 < 2\theta < 105°$, $\Delta 2\theta = 0.02°$, 16 h scan. Nominal resolution for both instrumental setups used is 0.08° 2θ (Mo Kα_1) for the LaB_6 peak at ca. 21.3° (2θ).

Standard peak search methods and indexing of the first lines ($2\theta < 30°$) by TOPAS-R (Bruker AXS, 2005) allowed determination of the cell parameters (see Table 1). Systematic absences, density, and geometrical considerations indicated space groups $P2_1/c$, $P2_1/c$, *Pccn*, *P*-1, *C*2/*c*, and *Cmca* for compounds **1**, **2**, **3**, **4**, **6**, and **8**, respectively. Successful structure solutions and refinements confirmed these cell and space group choices. The structural models employed in the final whole-pattern Rietveld-like refinement were determined ab initio by the simulated annealing technique implemented in TOPAS-R using (partially flexible) rigid bodies for the Bim ligand, helping convergence and stability: two free conformational parameters were used, i.e., the torsional angles about the N−CH_2 bonds. The background contribution was modeled by a polynomial function; preferred orientation correction was necessary

Table 2. Crystal Data and Structure Refinement Parameters for the Cadmium Derivatives **6** and **8**

	6	**8**
empirical formula	$C_7H_8Br_2CdN_4$	$C_{18}H_{19}O_2CdN_8$
fw	420.39	520.80
cryst syst	monoclinic	orthorhombic
space group	*C*2/*c*	*Cmca*
unit cell dimensions		
a (Å)	14.682(1)	9.399(1)
b (Å)	10.898(1)	17.9007(4)
c (Å)	14.786(1)	12.762(1)
α, deg	90	90
β, deg	64.795(5)	90
γ, deg	90	90
V (Å^3)	2140.6(3)	2147.2(2)
Z	8	16
D_c (Mg m^{-3})	2.6088	1.6111
abs coeff (mm^{-1})	24.825	8.519
F(000)	1568.0	1040.0
2*θ* range	9−105	5−105
indexing GoF	51.5	21.0
R_p, R_{wp}	0.090, 0.115	0.047, 0.148
R_{Bragg}	0.042	0.049
goodness-of-fit	1.76	3.136

for **1**, **3**, **5**, and **8**, and a single isotropic B_M value was refined for each compound (lighter atoms were arbitrarily assigned a $B = B_M + 2.0$ Å^2 value). Peak shapes were described by the fundamental parameters approach with anisotropic peak broadening only for compound **2**. The final Rietveld refinement plots are shown in Figure S1 in the Supporting Information, while Tables 1 and 2 contain the relevant crystal data and data analysis parameters for the zinc and cadmium complexes, respectively.

Thermodiffractometric Analysis and Evaluation of the Thermal Strain Tensors. Thermodiffractometric experiments were performed in air from 25 to ca. 300 °C using a custom-made sample heater, assembled by Officina Elettrotecnica di Tenno, Ponte Arche, Italy. Diffractograms at different temperatures (with steps of 20 °C) were recorded in the range 9−26°, 8−27°, and 9−22° 2*θ* for compounds **2**, **4**, and **6**, respectively. These regions were chosen for the presence of particularly significant peaks. The diffraction data were treated as previously reported[1] with a parametric analysis (imposing linear dependence).

Results and Discussion

Synthesis and Spectroscopy. The complexes **1**−**8** were synthesized in alcohols at room temperature. All complexes are stable at room temperature and, with exception of **8**, not soluble in water and hydroalcoholic and chlorinate solvents. Only species **1**−**3** were found to be moderately soluble in DMSO, their oligomeric or polymeric nature being possibly affected by DMSO solvation. It is worth noting that for both bromide salts employed here ($ZnBr_2$ and $CdBr_2$) two different adducts formed depending on the ligand to metal ratio employed. Such versatility has not been observed when metal chlorides and acetate were used.

The IR spectra of these solid species typically show several bands usually associated with the organic ligand: signals of weak and medium intensity at ca. 3000 cm^{-1} (C−H stretching modes) and other more intense bands between 1600 and 1500 cm^{-1} (typical of ring breathing).

Somewhat more informative are the far-IR spectra of the halide (X) complexes: in **1** we assign the two strong bands around 300 cm^{-1} to symmetric and asymmetric zinc−chloride stretching modes, whereas a medium intensity band at ca. 220 cm^{-1} can be ascribed to a Cl−Zn−Cl bending mode. As expected, the Zn−X stretching absorptions are shifted to lower energies on passing from Zn−Cl to Zn−Br [ν(Zn−Br) 260 cm^{-1}]. The pattern of far-IR absorption bands in **3** could not be easily assigned and suggests a different chemical environment for the Br$^-$ ion (vide infra).

The Cd−Cl stretching frequencies in **5** are shifted to lower frequencies with respect to those found in analogous bis(pyrazolyl)methane−$CdCl_2$ adducts.[15] The absorptions observed in the far-IR region are similar to those indicated for chlorine-bridged metal(II) dimers and oligomers. This fact, together with the insolubility of the sample, suggests a polynuclear structure, which unfortunately could not be proved by our XRPD measurements (vide infra). Analogously, Cd−Br stretching frequencies are absent in the spectra of derivatives **6** and **7** in the region 300−200 cm^{-1}, in reasonable agreement with a polynuclear Br-bridged structure (as found for **6** by XRPD).

In the case of carboxylate derivatives **4** and **8** it is generally accepted that it is possible to distinguish between ionic, unidentate, chelating bidentate, or bridging bidentate groups on the basis of the $\Delta = \nu_a(COO) - \nu_s(COO)$ value. The following trend has been generally reported in the literature

$$\Delta_{unidentate} > \Delta_{ionic} > \Delta_{bridging\ bidentate} > \Delta_{chelating\ bidentate}$$

where Δ_{ionic} is ca. 160−170 cm^{-1} for acetates. In our Bim derivatives **4** and **8** we predict a unidentate coordinating behavior of $RCOO^-$, Δ being ca. 220 and 215 cm^{-1}, respectively.[16]

In the ^{1}H NMR spectra (recorded in DMSO-d_6 for compounds **1**−**3** and D_2O for **8**) all the signals corresponding to Bim protons are only very slightly displaced toward lower fields upon coordination, as already seen in other zinc and cadmium derivatives of N-donor ligands.[17] Whether the integrity of the Bim−metal cores present in the solids (see below) is (at least partially) maintained upon dissolution of these polynuclear complexes in DMSO (or water) cannot be ensured since their extensive solvation might force significant N-ligand dissociation by these strongly coordinating solvents.

Crystal Structures of Zinc Derivatives 1−**4.** Crystals of **1** and **2** are strictly isomorphous and contain dimeric $[ZnX_2(Bim)]_2$ molecules (X = Cl for **1**, Br for **2**) located about a crystallographic inversion center of the monoclinic $P2_1/c$ space group (see Figure 1). The zinc ions are coordinated in a pseudotetrahedral fashion by two terminal halide ligands [Zn−Cl1 = 2.211(4) and Zn−Cl2 = 2.219(4) Å; Cl1−Zn−Cl2 118.0(2)° in **1**; Zn−Br1 = 2.353(4) and Zn−Br2 = 2.400(5) Å; Br1−Zn−Br2 114.9(2)° in **2**] and two nitrogen atoms [Zn−N1 = 2.05(3)/2.02(5) and Zn−N4 = 2.02(1)/2.05(2) Å for **1** and **2**, respectively] from two

(15) Pettinari, C.; Gioia Lobbia, G.; Lorenzotti, A.; Cingolani, A. *Polyhedron* **1995**, *14*, 793−803.
(16) Deng, Y.; Wang, R.-J.; Ding, T.-Z.; Li, Y.; Sun, S.-Q.; Feng, Y.-P.; Zhao, Y. F. *Polyhedron* **2001**, *20*, 291−295.
(17) Bovio, B.; Cingolani, A.; Pettinari, C.; Gioia Lobbia, G.; Bonati, F. *Z. Anorg. Allg. Chem.* **1991**, *602*, 169−172.

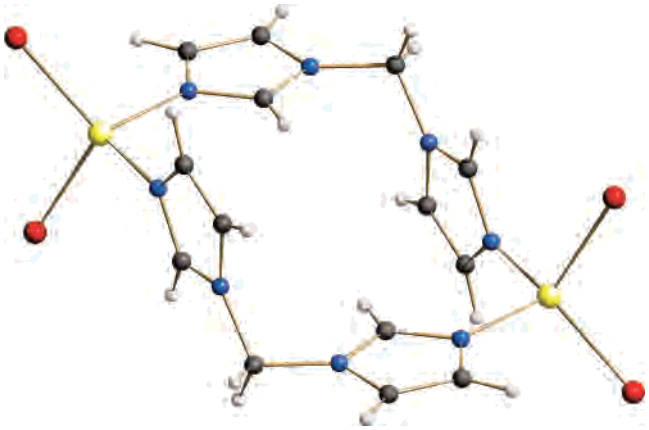

Figure 1. Schematic drawing of the molecular structure of the centrosymmetric $[ZnBr_2(Bim)]_2$ dimer, **2**. Zinc atoms are shown in yellow and bromine atoms in red. In **1**, nearly identical molecules are present with the bromine ions substituted by chloride ligands.

different Bim ligands. The latter bridge zinc atoms which are about 8.15 Å apart and generate N1−Zn−N4 angles of about 101.8(5)°/103.2(9)°. As anticipated in our previous paper, in order to quantitatively address the stereochemistry of Bim, we found it useful to employ two torsional angles, τ_1 and τ_2, defined by the $C_N-N-C_{H2}-N$ sequence, i.e., those involving the orientation of each imidazole ring with respect to the N−methylene bridge (see Chart 1). Note that with this choice $\tau_1 = \tau_2$ means rigorous C_2 symmetry while $\tau_1 = -\tau_2$ defines the C_s one. With these definitions in mind we observe that $[ZnX_2(Bim)]_2$ molecules show Bim ligands with $\tau_1 = 108.8°/110.5°$ and $\tau_2 = -52.4°/-52.0°$ for **1** and **2**, respectively, thus possessing a relative conformation far from both C_2 and C_s symmetry although closer to the latter.

Crystals of **3** contain polymeric one-dimensional chains of $[Zn(H_2O)_2(Bim)_2]^{2+}$ formulation surrounded by Br^- ions (granting electroneutrality) and crystallization water molecules (see Figure 2). The metal atoms lie on a special position (a two-fold axis aligned along *c*), as the lattice water molecules do. Each Zn atom lies in a distorted octahedral arrangement of a ZnN_4O_2 chromophore with Zn−N distances (from four different Bim ligands) of 2.12(2) and 2.14(2) Å and much longer contacts (2.96 Å) with two loosely coordinated (cis) water molecules. Accordingly, the trans N1−Zn−N1 angle is bent away from the ideal value of 180°, down to 139.9(5)°, confirming the weakness of the Zn−O interactions. The polymeric chains, built on Zn_2Bim_2 rings (similar to those found in **1** and **2**) hinged about the common zinc atoms (which lie ca. 8.52 Å apart), extend through the lattice along the [110] direction and possess *12* rod group symmetry. The τ_1 and τ_2 values (85.3° and −81.7°, respectively) speak for a nearly ideal C_s symmetry of the Bim ligand. As anticipated, these positively charged chains are embedded in a Br^-/H_2O matrix, interacting through significant H-bond contacts (Br···O 3.21−3.26 Å).

Crystals of **4** contain polymeric $[Zn(CH_3COO)_2(Bim)]_n$ molecules, extending in the crystal lattice along the crystallographic *c* direction of a triclinic lattice (see Figure 3). The zinc ions are coordinated in a pseudotetrahedral fashion by two terminally bound acetate ligands [Zn−O1a and Zn−O1b = restrained at 2.00(3) Å; O1a−Zn−O1b = 95.0(6)°] and two nitrogen atoms [with Zn−N1 and Zn−N4 restrained at 2.00(3) Å, N−Zn−N = 118.5(7)°] from two different Bim ligands. The swinging oxygen atoms of the acetate groups lie about 2.81 and 3.07 Å away from the metal ions (but trans to each other with respect to the metal), thus manifesting a clear acetate monodentate coordination mode (confirming IR observations). As in the previously described species, zinc atoms connected by the Bim bridge are rather far apart (here at about 9.35 Å) with the Bim ligands showing τ_1 and τ_2 angles of 92.6° and −103.3°, respectively, thus possessing a relative conformation of approximate C_s symmetry. Note that species **4** was prepared as a solid material of limited crystallinity; thus, if no restraints were applied to force Zn−N distances to nearly equivalent values, a (probably) chemically unmeaningful spread of metal-to-ligand distances is derived. Nevertheless, more than ever, we point out that through XRPD the connectivity, intermetallic distances, crystal packing, and ligand conformational features are reasonably determined while other more subtle details are missing. Needless to say, bad data are better than no data at all.

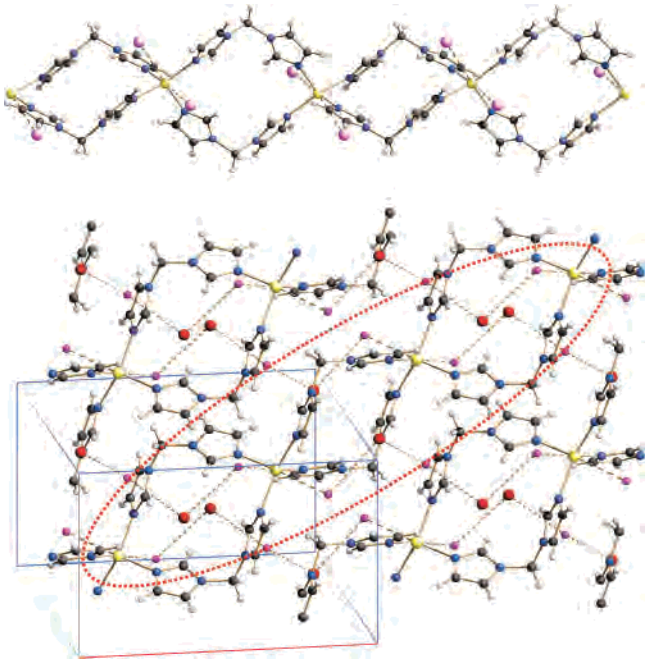

Figure 2. Schematic drawing of (a) a portion of the one-dimensional chain present in $ZnBr_2(Bim)\cdot 3H_2O$, **3**, and (b) the crystal packing (viewed approximately down *c*), highlighting the hydrogen-bond network and loose Zn−O contacts with fragmented lines. The ellipse shows the polymer chain running in the (110) direction. Zn atoms are shown in yellow, bromide ions in red, and (water) oxygens in magenta.

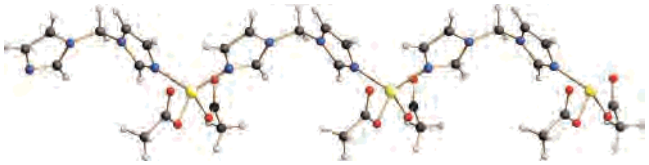

Figure 3. Schematic drawing of the portion of the one-dimensional chain present in $[Zn(CH_3COO)_2(Bim)]_n$, **4**. The polymer elongates in the *a* direction. Zinc atoms are shown in yellow and acetate oxygen atoms in red.

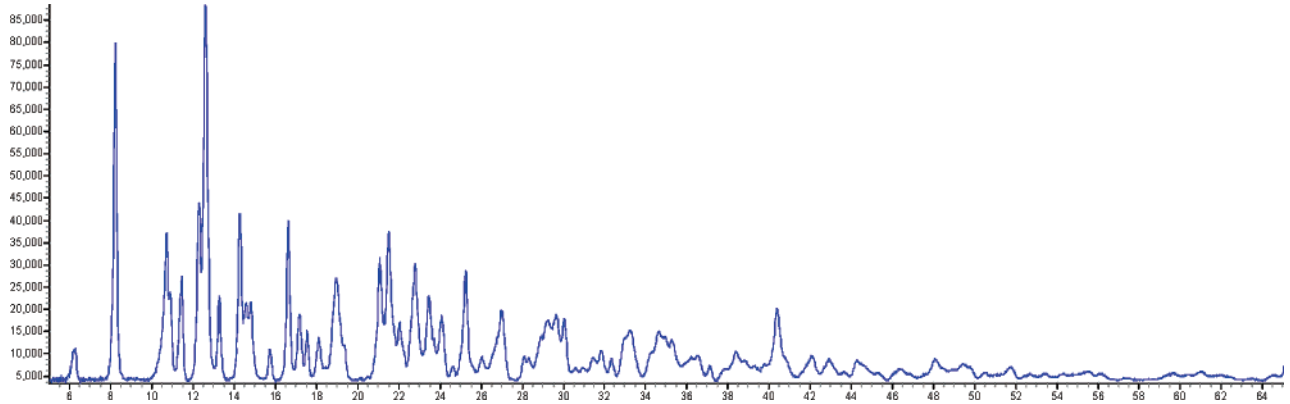

Figure 4. Raw X-ray diffraction data for $Cd_2Cl_4(Bim)_2(H_2O)(EtOH)$, **5**.

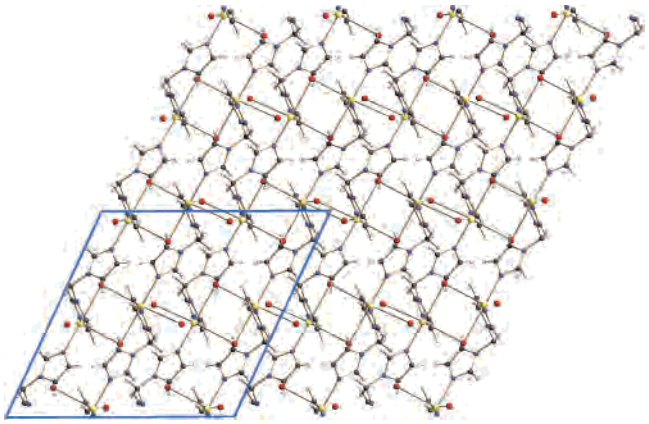

Figure 5. Schematic drawing of a portion of the three-dimensional polymer $[CdBr_2(Bim)]_n$, **6**, viewed down (010). Horizontal axis: *c*. Cadmium atoms are shown in yellow and bromine atoms in red.

Crystal Structures of Cadmium Derivatives 5, 6, and 8. The complexity of the X-ray powder pattern of compound **5** prevented the full assignment of the structural features of this species. However, as shown in Figure 4, the rich XRPD trace speaks for a highly polycrystalline material (of still unknown structure). Aiming at obtaining further structural information, we performed ^{13}C CP-MAS NMR measurements, which indicated that *only one* crystallographically independent Bim ligand must be present (five, instead of six, resolved peaks at $\delta = 119.1$, 121.1, 128.9, 129.8, and 139.1 for the ring carbon atoms as well as the CH_2 resonance at $\delta = 53.6$ ppm are observed) and that indeed ethanol is hosted in the lattice ($\delta = 14.5$ and 56.9 ppm). Indexing of this XRPD trace indicated a possible orthorhombic *P* symmetry ($a = 28.91$ Å, $b = 16.28$ Å, $c = 9.31$ Å, and $V = 4384$ Å^3, $Z = 16$, $Z' = 2$), which apparently does not match the observation of the uniqueness of the Bim ligand. This can actually be explained by either the presence of a few diffraction peaks not belonging to species **5**, hampering detection of the true cell parameters, or assuming that in the NMR spectrum many more resonances are hidden below the observed peaks.

Crystals of **6** contain an extended three-dimensional framework of $[CdBr_2(Bim)]_n$ formulation with all atoms lying in the general position of the monoclinic *C*2/*c* space group (see Figure 5). Each cadmium ion is coordinated in a pseudooctahedral fashion by four μ_2-bridging bromide ligands [Cd−Br1 = 2.75(1) and 2.87(1) Å, Cd−Br2 = 2.83(2) and 2.93(1) Å, trans and cis Br−Cd−Br angles of 174.4(3)° and 101.8(2)−97.4(3)−95.4(3)−88.6(3)−81.5(3)°, respectively] and two nitrogen atoms (Cd−N1 = 2.53(2) and Cd−N4 = 2.23(2) Å) from two different Bim ligands in a cis position to one another [N1−Cd−N2 = 87.2(7)°]. In the crystal the shortest Cd···Cd interaction [4.12 and 4.25 Å] belongs to doubly bridged intermetallic contacts, while as expected much longer interactions are found for the metals connected by the μ-Bim ligands (9.14 Å). Using the notation defined above, in the $[CdBr_2(Bim)]_n$ polymer the Bim ligands possess a relative conformation of nearly C_s symmetry with τ_1 and τ_2 angles of 101.7° and −91.7°, respectively.

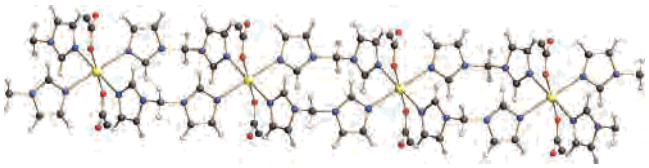

Figure 6. Schematic drawing of a portion of the one-dimensional polymer $[Cd(CH_3COO)_2(Bim)_2]_n$, **8**. The chain elongates in the *a* direction. Cd atoms are shown in yellow and acetate oxygen atoms in red.

Crystal of **8** contain one-dimensional neutral chains of $Cd(CH_3COO)_2(Bim)_2$ formulation with the metal atoms showing a trans CdN_4O_2 pseudooctahedral geometry and acetate ligands connecting to the metals (as found in **4**) only through *one* oxygen atom (see Figure 6). In *Cmca*, Cd ions lie on a *2*/*m* symmetry site while each acetate lies completely on the mirror plane normal to *a*; also, the Bim ligands are bisected by these planes and, consequently, show crystallographically imposed C_s symmetry ($\tau_1 = -\tau_2 = 87.8°$). Relevant bond distances are Cd−N 2.336(5), Cd−O 2.43(1) Å and (doubly bridged by Bim ligands) Cd···Cd 9.40 Å (the *a* axis). It is worth noting that this poly spiro 1D polymer (of *2*/*m* rod symmetry) closely resembles that of $[Zn(H_2O)_2(Bim)_2]^{2+}$, **3**, which only differs by the cis (and not trans) O-coordination at the metal atoms and the not collinear (but slightly zigzagging) disposition of the metal ions (Zn···Zn···Zn 150.2°).

Comparative Structure Analysis. The structures reported above share some similar features: the Bim ligands are invariably found to bridge metal atoms at rather large distances (>8 Å, favoring, in principle, large cavities if suitably arranged in space) and possess rigorous (or nearly

Table 3. Synoptic Collection of Relevant Structural and Stereochemical Features of Compounds **1**, **2**−**4**, **6**, and **8**

	1	**2**	**3**	**4**	**6**	**8**
topology	0D	0D	1D	1D	3D	1D
chromofore	ZnN_2Cl_2	ZnN_2Br_2	ZnN_4O_2	ZnN_2O_2	CdN_2Br_4	CdN_4O_2
geometry	tetrahedral	tetrahedral	octahedral	tetrahedral	octahedral	octahedral
M−N, Å	2.02−2.05	2.02−2.05	2.12−2.14	2.01−2.03[a]	2.23−2.53	2.33
M−(O,Cl,Br), Å	2.21−2.22	2.35−2.40	2.97	1.99−2.00[a]	2.74−2.93	2.43
M−Bim−M, deg	8.16	8.15	8.52	9.36	9.14	9.40
N−M−N, deg	101.8	103.2	95.8	118.5		90
			96.9			180
			139.9			
τ_1, deg	108.5	110.95	85.3	92.6	100.7	87.8
τ_2, deg	−52.4	−52.0	−81.7	−103.3	−91.7	−87.0
idealized Bim symmetry	C_1	C_1	C_s	C_s	C_s	C_s
M site symmetry	1	1	2	1	1	2/*m*

[a] Restrained values (see text).

so) C_s symmetry (see Table 3). The free ligand (in the solid state[11]) crystallizes in the $P2_12_12$ space group and, lying on a two-fold axis, shows a C_2 conformation. This type of conformer has also been observed in a number of coordination polymers, while more rarely[10a] the C_s conformers are found. Interestingly, in the $[M(Bim)_3](ClO_4)_2$ (M = Zn, Cd) species[10a] both conformers coexist. Interestingly and apparently with no evident energetic or stereochemical motivation none of the species proposed in this contribution shows a C_2 conformation, which was found to be nearly ubiquitous in the organometallic Sn(IV) one-dimensional polymers.[1]

This variety of conformations and, to a lesser extent, the ionic radii of Zn(II) and Cd(II) are responsible for the markedly different intermetallic distances collected in Table 3; if, however, structures containing similar fragments [as $Cd_2(Bim)_2$ rings] are compared, then very similar intermetallic contacts are observed: ca. 9.40 Å in **8** and $[Cd(Bim)_2(N_3)]_n$,[10a] which share markedly different crystal symmetries.

Apparently, none of these species possesses large cavities capable of hosting labile solvent or gaseous molecules (with the exception of the still structurally uncharacterized compounds **5** and **7** in which alcohol molecules are present), indicating that the flexibility of the Bim ligand probably allows formation of dense crystal packings, which other (more rigid) linkers (such as aromatic polycarboxylates[2] or polyazolates[18]) do not favor. However, the observed conformational freedom may be actively used in the preparation of coordination polymers of the flexible type if a suitable combination of metals and counterions is found. Indeed, similar flexible compounds with polypyridines are known.[19]

Thermal Evolution and Thermal Strain Tensors. Apart from the two cyclic oligomers of the $[ZnX_2(Bim)]_2$ type and from the 3D $CdBr_2(Bim)$ polymer all these species are based on 1D polymeric chains packed in space as more or less parallel bundles. With the aim of learning some information on the forces acting among these chains, most of the van der Waals type, we performed in situ thermodiffractometric measurements of three selected compounds taken as representative of each class: $[ZnBr_2(Bim)]_2$ (**2**, 0D), $[Zn(CH_3COO)_2(Bim)]_n$ (**4**, 1D), and $[CdBr_2(Bim)]_n$ (**6**, 3D).

Compound **2** shows a relevant thermal strain anisotropy (Figure 7, top) with the *a* and *b* axes expanding with temperature ($(1/a)(\partial a/\partial T) = 4.1 \times 10^{-5}$ and $(1/b)(\partial b/\partial T) = 3.9 \times 10^{-5}$ K^{-1}), while *c* contracts ($(1/c)(\partial c/\partial T) = -1.1 \times 10^{-5}$ K^{-1}). This is quite unusual for a molecular crystal and could be related to the presence of a soft "breathing mode" of the cyclic molecules, which upon heating are slightly squeezed and flattened.

The data shown in Figure 7 for the one-dimensional chain of **4** are slightly more complex to interpret; basically, once can notice the substantial constancy of the *c*-axis value (along which the covalent polymer chains run), thus suggesting that the softer directions are nearly normal to it, i.e., among chains interacting by weak(er) H···H van der Waals contacts. While this result was indeed expected, our measurement quantitatively assessed the relative importance of the packing forces in the crystals of **4** as witnessed by *average* thermal expansion coefficients of $(1/a)(\partial a/\partial T) = 6.0 \times 10^{-5}$, $(1/b)(\partial b/\partial T) = -2.1 \times 10^{-5}$, and $(1/c)(\partial c/\partial T) = -0.8 \times 10^{-5}$ K^{-1}.

The last material studied, polymer **6**, has a 3D framework with significantly different intermetallic contacts, i.e., those bridged by bromine atoms or Bim ligands. The thermal expansion coefficients derived from the lattice parameter variations shown at the bottom of Figure 7 ($(1/a)(\partial a/\partial T) = 1.7 \times 10^{-5}$, $(1/b)(\partial b/\partial T) = -1.6 \times 10^{-5}$, and $(1/c)(\partial c/\partial T) = 5.3 \times 10^{-5}$ K^{-1}) show expansion on *a* and *c* while *b* slightly shrinks upon heating. With reference to the proposed three-dimensional structural model (and to the tensor representation shown in Figure 9) we tentatively suggest that the more flexible moiety is the polymeric sequence of Cd_2Br_2 rhombi (aligned with *c*) while the small thermal expansion coefficient of the *b* axis speaks for a substantial rigidity of the Cd−Bim−Cd links, which connect (in an oblique manner) the *spiro*-Cd_2Br_2 polymeric chains stacked along [0 1 0]. A similar rigidity driven by the Bim bridges has been discussed in ref 1.

(18) Hayashi, H.; Côté, A. P.; Furukawa, H.; O'Keeffe, M.; Yaghi, O. M. *Nat. Mater*. **2007**, doi:10.1038/nmat1927.

(19) See, for example: Fletcher, A. J.; Thomas, K. M.; Rosseinsky, M. J. *J. Solid State Chem.* **2005**, *178*, 2491−2510. Wang, S.; Xing, H.; Li, Y.; Bai, J.; Pan, Y.; Scheer, M.; You, X. *Eur. J. Inorg. Chem.* **2006**, 3041−3053. Hiroshi, K.; Hiroshi, N.; Atsushi, K.; Shunsuke, O.; Yoshiyuki, H.; Hideki, T.; Hirofumi, K.; Katsumi, K. *Nippon Kagaku Koen Yok.* **2006**, *86*, 457. Casellas, H.; Roubeau, O.; Teat, S. J.; Masciocchi, N.; Galli, S.; Sironi, A.; Gamez, P.; Reedijk, J. *Inorg. Chem.* **2007**, *46*, 4583−4591.

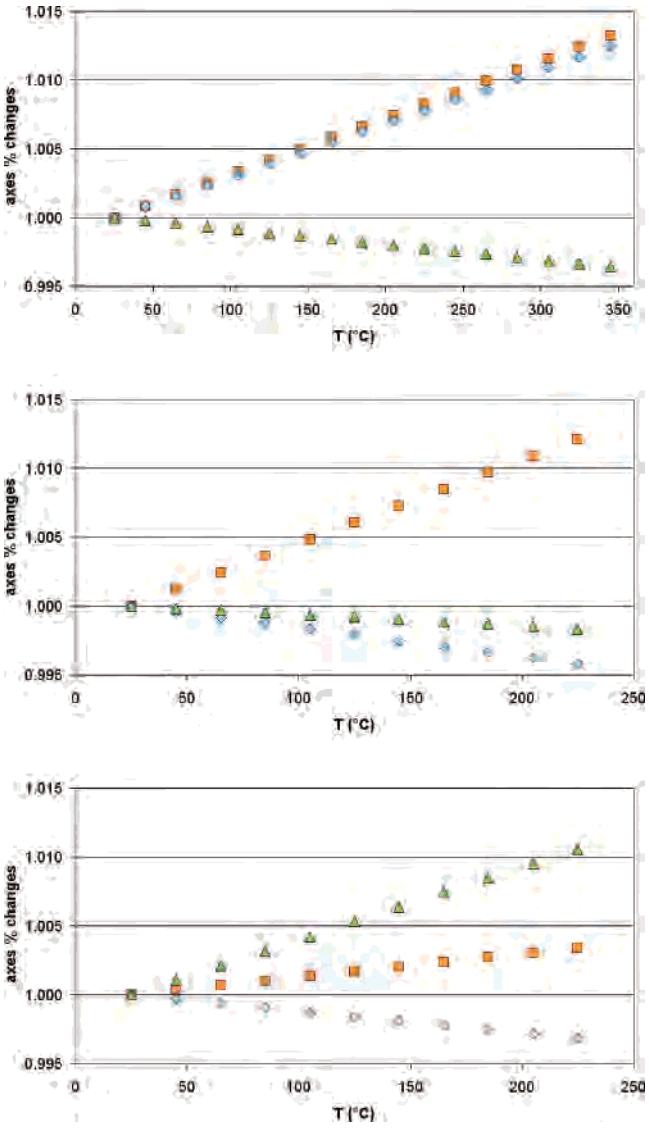

Figure 7. Relative thermal variations of cell axes of (top to bottom) $[ZnBr_2(Bim)]_2$, **2** (note the evident contraction of the *c* axis on heating), (b) $[Zn(CH_3COO)_2(Bim)]_n$, **4** (both *b* and *c* axes contract on heating), and (c) $[CdBr_2(Bim)]_n$, **6** (*b* shrinks): $a = \square$, $b = \diamond$, $c = \triangle$.

Conclusions

The Bim ligand, which has rarely been employed in the construction of polynuclear coordination complexes, has been reacted with zinc and cadmium halides and acetates. The derived adducts, with a ligand-to-metal ratio of 1:1 or 2:1, have been characterized by analytical and spectroscopic methods and, above all, less conventional powder diffraction techniques. The crystal and molecular structures derived there from unambiguously showed that cyclic (zero-dimensional) oligomers or extended 1D or 3D polymers can be formed depending on the metal and counterion properties.

The Bim ligand, which possesses two torsional degrees of freedom (about the two CH_2-N bonds), was found to preferentially adopt a pseudo-C_s symmetry conformation, although a few slightly less symmetric cases [the Zn(II) oligomers] have been also detected. Whether this is a systematic or occasional stereochemical preference cannot be determined on the basis of our data alone, thus requiring a deeper structural and computational study and variation of the metals and overall stoichiometry and crystal packings. Work can be anticipated in the direction of understanding these aspects and has recently been communicated.[20] To this goal, other derivatives with different counterions (iodides, nitrates, fluoroborates/phosphates, etc.) will be prepared in the search for general stereochemical rules to be adopted in engineering 3D coordination networks of the porous type, useful in storage and separation methods of environmentally relevant gases.

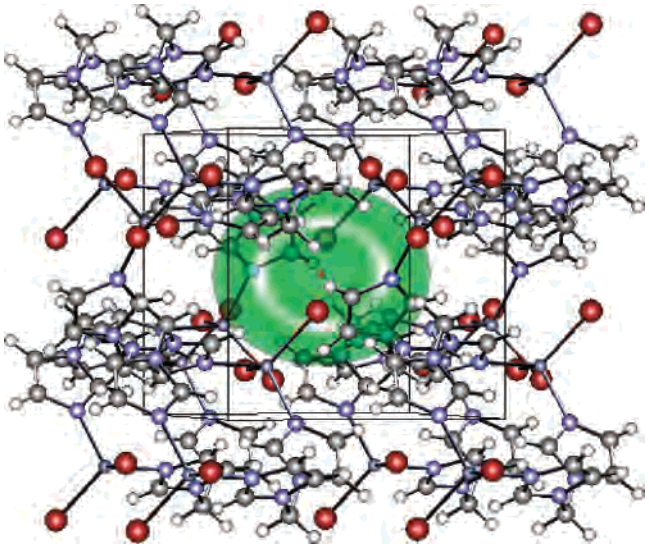

Figure 8. Thermal strain tensor of $[ZnBr_2(Bim)]_2$, **2**, isooriented with its crystal packing, viewed down the contracting principal axis. Horizontal axis: *a*. Green portions indicate expansion, while the red one (central red dot) highlights (minor) contraction directions (approximately aligned with *c*).

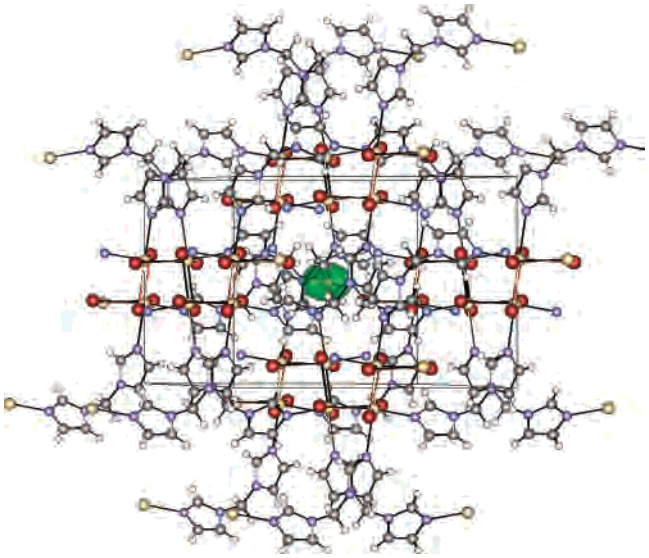

Figure 9. Thermal strain tensor of $[CdBr_2(Bim)]_n$, **6**, isooriented with its crystal packing, viewed down the longest principal axis (almost parallel to *c**). Horizontal axis: *a*. Green portions indicate expansion, while the red one highlights (minor) contraction directions (approximately aligned with *b*).

(20) Masciocchi, N.; Galli, S.; Figini Albisetti, A.; Sironi, A.; Di Nicola, C.; Pettinari, C. QIES-06, 12×bb Reunión Científica Plenaria de Química Inorgánica, Barcelona, Spain, 2006.

Finally, use of thermodiffractometry on selected examples has shown that using static (isothermal) measurements and different XRPD patterns measured at different temperatures not only the anisotropic lattice-parameters thermal expansion coefficients and the three-dimensional thermal strain tensor can be derived but also that dynamics of the molecules in these soft lattices can be tentatively inferred.

Acknowledgment. This work was supported by the Italian MUR (PRIN2006: "Materiali Ibridi Metallo-Organici Multifunzionali con Leganti Poliazotati"). The Fondazione Provinciale Comasca is acknowledged for partial funding. We thank Dr. Simona Galli (University of Insubria) for helpful discussions.

Supporting Information Available: Rietveld refinement plots for compounds **1**−**4**, **6**, and **8**. This material is available free of charge via the Internet at http://pubs.acs.org. Crystallographic data (excluding structure factors) for the structures reported in this paper have been deposited with the Cambridge Crystallographic Data Center as supplementary publication no. CCDC 655202−655207. Copies of the data can be obtained free of charge on application to the Director, CCDC, 12 Union Road, Cambridge, CB2 1EZ, UK (Fax: +44-1223-335033; e-mail: deposit@ccdc.cam.ac.uk or http://www.ccdc.cam.ac.uk).

IC7015319